Synchronization of chaotic maps through a noisy coupling channel with application to digital communication

Ali A. Minai and Tirunelveli Anand
Department of Electrical and Computer Engineering and Computer Science, University of Cincinnati, Cincinnati, Ohio 45221-0030
(Received 10 April 1998; revised manuscript received 9 July 1998)

While synchronization of coupled chaotic systems has been the subject of intensive research, many issues in this field remain open. Among the most important of these is robustness to channel noise: Can synchronization be guaranteed even if the coupling channel is noisy? This issue is of great significance if coupled chaotic systems are to find use in communications, as has been suggested by some researchers. In this paper, we show that chaotic maps can indeed be synchronized reliably even in the presence of some types of channel noise, simply through the use of thresholding. This synchronization is reliable and rapid enough to be useful in digitally implemented systems with finite precision. We also outline a simple communication scheme using the proposed synchronization method. [S1063-651X(99)00901-0]

PACS number(s): 05.45.Vx

I. INTRODUCTION

Following the pioneering work by Pecora and Carroll [1,2], there has recently been a surge of interest in the issue of synchronization in chaotic systems [3–5]. While most work has focused on continuous-time systems, there are also some studies of synchronization between coupled discrete-time maps [6–9,5,10–15]. Large systems of coupled maps have been investigated in detail by several researchers and a variety of complex behaviors, including clustering and synchronization, have been found [16–23].

A major concern in all schemes for synchronizing coupled oscillators is robustness against noise in the channel carrying the coupling signal. It is well known that, for chaotic oscillators, synchronization can be disrupted intermittently or permanently in drastic ways by even a small amount of additive noise [24,12,25]. In some cases, it is possible to overcome this by increasing the strength of coupling, leading to the notion of *high-quality synchronization* [26,12].

In recent reports [27,28] we have shown that identical chaotic maps of a certain type can be synchronized when driven by the same random two-level switching signal. Since the drive signal is digital in nature, additive channel noise can be removed from it by simple thresholding, making the synchronization robust against such noise. In this paper we demonstrate the utility of this idea. The rest of this paper consists of four sections. In Sec. II we look at synchronization between uncoupled maps driven by an externally supplied digital signal. This extends our previous work reported in [27]. In Sec. III we develop results for synchronization between coupled maps with internally derived digital signals and these results are analyzed in Sec. IV. Finally, in Sec. V, we outline a possible application for the system in masked communications.

II. SYNCHRONIZATION OF MAPS VIA RANDOM DRIVING

We begin with a discussion of how two identical maps of a certain form synchronize when driven by a common digital signal. This extends and refines the results presented in [27,28]. The map we use is the difference of two hyperbolic tangents

$$x_{t+1}=f(x_t,u_t)=\tanh[\mu(ax_t+u_t)]-\tanh[\mu bx_t], \quad (1)$$

where u_t is an external input. If $u_t=0 \ \forall \ t$, increasing μ with fixed a and b leads to chaotic dynamics through period doubling [29,30]. If μ,a, and b are such that the autonomous map is chaotic, applying a fixed input $u_t=u \ \forall \ t$ leads to a period-halving cascade with increasing u, culminating in a period-2 regime [31]. Thus, for any fixed u, the map $f(x,u)$ has a definite Lyapunov exponent $\lambda(u)$, which is positive for small u (except in periodic windows) and negative for larger u [27].

Now consider two identical $f(x,u)$ maps driven by the random telegraph signal (RTS) $u_t\in\{L,H\}$, where $0\leqslant L<H$:

$$x^1_{t+1}=f(x^1_t,u_t)=\tanh[\mu(ax^1_t+u_t)]-\tanh[\mu bx^1_t], \quad (2)$$

$$x^2_{t+1}=f(x^2_t,u_t)=\tanh[\mu(ax^2_t+u_t)]-\tanh[\mu bx^2_t]. \quad (3)$$

The input takes on the value L with probability p and H with probability $1-p$. Over a wide range of parameter settings, the two maps synchronize within a short period [27]. This is the result of *coalescence*, a phenomenon analyzed in some detail by others [32,33,7,34–36]. For synchronization to occur, the system and the input signal must satisfy some conditions, which we discuss next.

Define $e_t=x^1_t-x^2_t$ as the error phase variable for the system, with the dynamics

$$e_{t+1}=F(e_t,x^1_t,u_t)=f(x^1_t,u_t)-f(x^1_t-e_t,u_t).$$

Clearly, $e_t=0$ is an invariant manifold for the system's dynamics. The stability of this manifold is determined by the transverse conditional Lyapunov exponent (CLE) along the (x^1_t,u^t) trajectory on the $e_t=0$ manifold. This is given by

$$\Lambda = \langle \ln|\partial F(e_t, x_t^1, u_t)/\partial e_t| \rangle = \langle \ln|f'(x,u)| \rangle$$
$$= \lim_{T\to\infty} \frac{1}{T} \sum_{t=\tau}^{\tau+T-1} \ln|f'(x_t^1, u^t)|, \quad (4)$$

where the partial derivative is evaluated along $e_t = 0$, angular brackets indicate averaging over the invariant distribution of (x_t^1, u_t) (if it exists), and $f'(x,u)$ is the derivative of $f(x,u)$ with respect to x. Thus the CLE of the synchronized trajectory for a time-varying u_t with a stationary distribution $P(u)$ can be approximated by $\Lambda = \int_u P(u)\lambda(u)du$. When $u_t \in \{L,H\}$ we get

$$\Lambda \approx p\lambda(L) + (1-p)\lambda(H). \quad (5)$$

Thus, by choosing p, L, and H appropriately, we can control the sign of the CLE for the synchronized trajectory [27]. (Note that our use of the term ''Lyapunov exponent'' for a stochastically driven system follows the practice of other researchers [32,33,7,34–36].) Also, as we have shown elsewhere, many other input distributions can also produce a negative CLE, entailing stable synchronization [28,31]. However, as discussed below, a negative CLE is not a sufficient condition for synchronization to emerge. In addition, in systems with finite precision, a negative CLE may also not be a necessary condition.

Assume that H is chosen such that $u_t = H$ puts the system in a period-2^k regime. There are then 2^k domains of attraction, one for each phase. If u_t were permanently set to H, our two-map system would have 2^{2k} stable configurations, but only 2^k of these would have identical phases. Thus, even though Λ would be negative, the maps could converge to a configuration with different phases, precluding synchronization. Now suppose that, after a long period with $u_t = H$, it is temporarily set to L, which puts the system in the single-band chaotic (mixing) regime. The only periodic configurations that are guaranteed to survive this episode are the 2^k phase-matched ones. All others are rapidly disrupted. Over several switches between $u_t = H$ and $u_t = L$, the system is driven to a phase-matched state by a process analogous to annealing, provided Λ is negative. The latter condition means that, even if the system does not continuously stay in the periodic regime long enough to converge precisely to a periodic configuration, such convergence dominates exponential separation *on average* and configurations close to being phase-matched are usually, but not always (see below), disrupted less quickly in the mixing regime than configurations with very different phases. Synchronization by this process is therefore a statistical phenomenon.

To illustrate these points, Fig. 1 shows how a set of 50 uniformly distributed initial conditions evolve in response to three types of driving inputs: (a) a RTS input $u_t \in \{0,1\}$ and $p = 0.5$, (b) a fixed input of $u_t = 0.0 \ \forall \ t$ (mixing only), and (c) a fixed input of $u_t = 1.0 \ \forall \ t$ (period-2 only). As expected, synchronization occurs only in the first case. In the case $u_t = 0.0$, the system evolves rapidly to the invariant density of the chaotic map, while for $u_t = 1.0$, it coalesces into two clusters, one for each phase of the period-2 cycle.

The above analysis gives us the following conditions on $u_t \in \{L,H\}$ for synchronization to emerge.

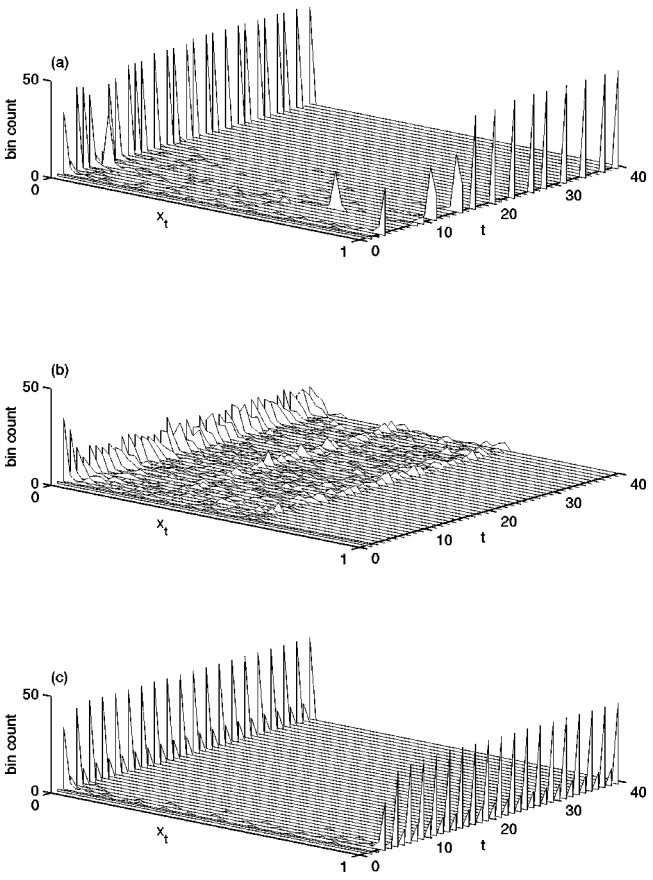

FIG. 1. Evolution of the state histogram for 50 identical maps with $\mu = 7.0$, $a = 5.0$, and $b = 1.0$. The initial condition for the kth map is given by $x_0^k = 0.02(k-1), k = 1, \ldots, 50$, giving a uniform distribution. All maps get identical inputs: (a) random telegraph signal input $u_t \in \{0,1\}$, (b) fixed input $u_t = 0 \ \forall \ t$ (chaotic phase), and (c) fixed input $u_t = 1 \ \forall \ t$ (periodic phase). Synchronization is apparent in (a), while in (c) the population divides into two groups corresponding to the phases of the period-2 orbit.

(i) The Lyapunov exponent of the random map $f(x,u)$ must be negative, i.e., the relative frequencies of L and H must be such that the resulting Λ value is negative. Note that a negative Λ does not preclude aperiodicity since it is only a conditional Lyapunov exponent (with respect to the random driving input u_t). The total (x_t, u_t) system is still aperiodic, with the randomness of u_t supplying the volume expansion necessary to prevent collapse to a periodic attractor. Qualitatively, the dynamics of x_t consists of alternating variable length episodes of chaotic and periodic evolution.

(ii) L must be chosen to put the system in the single-band chaos (mixing) regime and H to put it in a low-period cyclic regime. Choosing H is typically a simple matter since the period-2 regime is very extensive. To choose L we need to know the value of u, designated u^*, where the mixing regime ends. When H is such that $f(x,H)$ is a period-2 orbit, the two basins for the phases of the orbit are separated by the unstable fixed point $x^* = f(x^*,H)$. For maps with large μa, the tail of $f(x,u)$ is approximated accurately by $f(x,u) = 1 - \tanh(\mu b x)$, so that the fixed point is given by the solution of $x^* = 1 - \tanh(\mu b x^*)$ and is effectively independent of u. The boundary value of u for single-band chaos can then be stated as $u^* = u : f(0,u) = x^*$, which gives

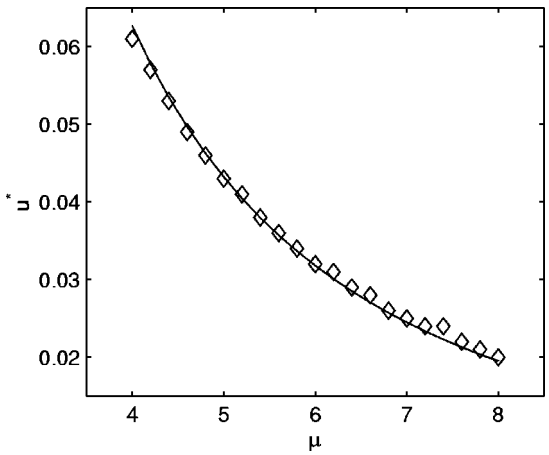

FIG. 2. Comparison of the empirically determined maximal L value needed for synchronization ($\diamond$) and the theoretical value given by u^* (solid line) for different values of μ. In all cases, $a=5.0$, $b=1.0$, and $p=0.5$.

$$u^* = \tanh^{-1}(x^*)/\mu.$$

Synchronization requires $L \leqslant u^*$. Figure 2 shows the actual empirically determined threshold value of L needed for reliable synchronization and the theoretical value u^* over a range of μ with $a=5.0, b=1.0$, and $p=0.5$, confirming the validity of the $L \leqslant u^*$ requirement. Analogous calculations can be made for the required value of L if $u=H$ puts the system in a 4- or 8-cycle.

While a negative CLE is essential for synchronization, it is not a sufficient condition. The emergence of synchronization also depends on localized characteristics of the dynamics and the maps. For example, suppose that the system switches into the mixing regime at time t_1 with $|e_{t_1}| = |x^1_{t_1} - x^2_{t_1}| = \delta$, where δ is very small, and remains there for T steps before switching back into the periodic regime. If T is not too large, the growth of the absolute error is approximately given by

$$|e_{t_1+T}| \approx \left[\prod_{t=t_1}^{t_1+T-1} |f'(\xi_t, u_t)| \right] |e_{t_1}|,$$

where $\xi_t \equiv (x^1_t + x^2_t)/2$. Clearly, the extent to which the near synchronization survives this episode depends on the actual values of $f'(\xi_t, u_t)$ over the finite duration t_1 to t_1+T-1 and not so much on whether the overall conditional Lyapunov exponent is negative. The quantity

$$\hat{\Lambda}_T(x^1_{t_1}, x^2_{t_1}, u_{t_1}, \ldots, u_{t_1+T-1}) \equiv \frac{1}{T} \sum_{t=t_1}^{t_1+T-1} \ln|f'(\xi_t)|$$

is called a *local Lyapunov exponent* [7,34] and is, in this case, a random variable. The dynamics of synchronization depends also on the distribution of the local Lyapunov exponents, which in turn depends on the underlying map, the invariant disctribution of the dynamics, the initial conditions, and the realization of the driving random process.

To take a concrete example, consider two identical randomly driven logistic maps of the form

$$X^1_{t+1} = G(X^1_t, u_t) = (4-u_t) X^1_t (1 - X^1_t),$$

$$X^2_{t+1} = G(X^2_t, u_t) = (4-u_t) X^2_t (1 - X^2_t),$$

with $u_t \in \{0,1\}$ as before. We find that the Lyapunov exponent of the random maps (and thus the CLE of the synchronization manifold) becomes negative when $p < 0.95$ or so. However, synchronization only occurs for $p \approx 0.5$ or less. The reason is that, when $u_t = 0$ and the maps are in chaos, most values of $|\partial G(X,u)/\partial X|$ are quite large, implying large positive local Lyapunov exponents that grow rapidly with T. Thus synchronization cannot take hold if the system spends significant periods in the mixing regime and p must be made very small. Of course, synchronization would also not happen if $p=0$ since some mixing is essential. Thus the range of p in which logistic maps can synchronize is very narrow. In contrast, the $f(x,u)$ map that we use has $|\partial f(x,u)/\partial x| \ll 1$ over a large part of its domain even in the chaotic regime. This ensures that local Lyapunov exponents grow relatively slowly with T, which translates into a larger range of p over which synchronization happens. Thus, while the synchronization process we describe is quite general, it is more suitable for maps where expansion is localized in small regions of phase space during the mixing regime.

We term the synchronization process discussed above *coalescence-based synchronization* to distinguish it from methods based on differential feedback [6,7,9,11,15]. The dependence of coalescence on local Lyapunov exponents makes it susceptible to two phenomena that occur also in feedback-based schemes to a lesser degree. These are *attractor bubbling* [24] and *on-off intermittency* [32,33,37,25]. However, when the underlying system is implemented digitally with finite precision (e.g., a digital communications system or an encryption program), both bubbling and intermittency are mitigated in broad regimes, as discussed below.

Attractor bubbling [24] occurs because the CLE for the synchronized trajectory can be negative without precluding finite-duration episodes of divergence between nearby trajectories due to positive local Lyapunov exponents. However, since the synchronized trajectory is the only long-term attractor, these episodes of desynchronization are always transient (if there are other attractors, one gets basin riddling [38]). Over time, the trajectory spends most of its time in or near the synchronized state, with rare interruptions. However, for systems implemented digitally, finite precision ensures that the desynchronization episodes cease once synchronization error has fallen below numerical precision. Empirical data shown in Fig. 3 indicate that, beginning with $|e_0| \sim O(1)$, the time, τ_ϵ needed for $|e_t|$ to fall below ϵ scales as $\tau_\epsilon \sim \log_{10}(1/\epsilon)$. Thus synchronization to even very high precision occurs within a short time.

On-off intermittency [32,33,37,25,39], which is the converse of bubbling, occurs when the CLE for the synchronized trajectory is positive, but there are finite-duration episodes of convergence between trajectories due to negative local Lyapunov exponents. This results in intermittent laminar and turbulent periods with characteristic scaling in their duration. Again, if the system is implemented with finite precision, these episodes of convergence can lead to actual synchronization when the trajectories of the two maps come closer than the system's precision. Thus finite-precision sys-

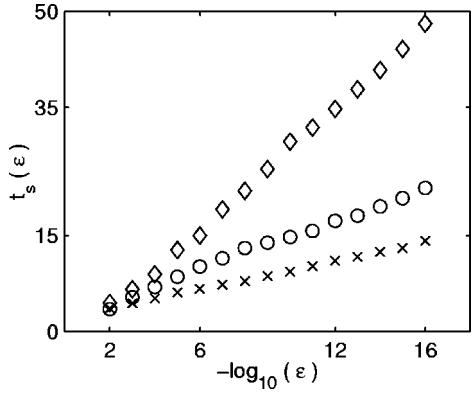

FIG. 3. First passage time t_s as a function of synchronization tolerance ϵ for x_t^1 and x_t^2. The system parameters are $\mu=7.0$, $a=5.0$, $b=1.0$, $u_t\in\{0,1\}$, and $p=0.3(\times)$, $p=0.5(\bigcirc)$, and $p=0.7(\diamond)$. All simulations were done at a precision of 10^{-16}. Note the linear dependence of t_s on $\log_{10}(1/\epsilon)$. Each point was averaged over 100 random initial conditions.

tems can synchronize even when the CLE is positive. However, such synchronization would be disrupted very easily by a small perturbation.

To summarize the discussion in this section, we can identify four broad regimes with respect to synchronization in systems with finite precision.

(i) An asynchronous regime with a positive CLE. Synchronization is not stable on average and local Lyapunov exponents are not able to drive the system into finite-precision synchronization.

(ii) An asynchronous regime with a negative CLE. Synchronization is stable on average, but either (a) local Lyapunov exponents during the mixing phase are too strongly positive to allow sufficient convergence of trajectories in general or (b) L does not place the system in the mixing regime.

(iii) A synchronous regime with a negative CLE. Synchronization is stable on average and trajectories converge to within any finite precision in linear time. This is the regime of primary interest and utility from our viewpoint. Note that while finite precision makes synchronization reliable and nonintermittent, synchronization is not *caused* by finite precision. That is shown by the linear dependence of synchronization time on numerical precision.

(iv) A synchronous regime with a positive CLE. Synchronization is unstable on average, but local Lyapunov exponents are sufficiently negative to drive trajectories closer than system precision. This requires that at least one Lyapunov exponent for the underlying system be negative. Some of these regimes are discussed below in the context of coupled maps.

III. SYNCHRONIZATION IN COUPLED MAPS

A natural question that arises from the foregoing results is whether the RTS input used for synchronizing can come from another aperiodic or chaotic map. In that case, one would have a synchronizable deterministic system. We study this issue by defining a system comprising a pair of identical two-dimensional maps. Each map, which we henceforth term an *oscillator,* is constructed from two $f(x,u)$ maps. The oscillators are termed the *drive oscillator* (d) and the *response oscillator* (r) and the system is given by

$$y_{t+1}^d = f_y(y_t^d, z_t^d) = \tanh\{\mu_y[Cy_t^d + \beta g(z_t^d, \theta_y)]\} - \tanh(\mu_y D y_t^d), \tag{6}$$

$$z_{t+1}^d = f_z(z_t^d, y_t^d) = \tanh(\mu_z\{Az_t^d + \alpha g[f_y(y_t^d, z_t^d), \theta_z]\}) - \tanh(\mu_z B z_t^d), \tag{7}$$

$$y_{t+1}^r = f_y(y_t^r, z_t^d) = \tanh(\mu_y\{Cy_t^r + \beta\phi[g(z_t^d, \theta) + \eta_t]\}) - \tanh(\mu_y D y_t^r), \tag{8}$$

$$z_{t+1}^r = f_z(z_t^r, y_t^r) = \tanh(\mu_z\{Az_t^r + \alpha g[f_y(y_t^r, z_t^d), \theta_z]\}) - \tanh(\mu_z B z_t^r), \tag{9}$$

where $\mu_y, \mu_z, A, B, C, D, \alpha$, and β are fixed parameters and $g(x,\theta)$ is a thresholding function that turns its analog argument x into a telegraph signal. It is defined as

$$g(x,\theta) = \begin{cases} L & \text{if } x < \theta \\ H & \text{if } x \geq \theta, \end{cases} \tag{10}$$

where L and H are constants and θ is a specified threshold. For simplicity, we assume that $\theta_z = \theta_y = \theta, L = 0.0$, and $H = 1.0$. We also assume $\alpha = \beta$, though a broad range of values can be used instead. The coupling between the oscillators is provided only by the $g(z_t^d, \theta)$ signal generated by the drive system. The signal received by the response system is $g(z_t^d, \theta) + \eta_t$, where η_t is zero-mean additive channel noise. We assume that there is no essential noise in the system, i.e., the noise is added only to the coupling signal, not to the system's phase variables. The function $\phi()$ is a threshold filter that attempts to recover the correct digital signal from the received noisy one:

$$\phi(x) = \begin{cases} L & \text{if } x < L + (H-L)/2 \\ H & \text{otherwise.} \end{cases} \tag{11}$$

This, of course, corresponds to optimal estimation for zero-mean noise with a symmetric distribution. If the additive noise has another known distribution, $\phi(x)$ can be defined appropriately. Clearly, if η_t has a distribution with bounded support $[-c, +c]$ (e.g., a uniform distribution), the system will be immune to its effect while $c < (H-L)/2$. If η_t has infinite support (e.g., a Gaussian distribution), but is largely confined to a narrow band of width less than $H-L$, synchronization will be robust with rare episodes of intermittency.

The system described in Eqs. (6)–(9) can be seen as two subsystems of the type discussed in Sec. II [Eqs. (2) and (3)]. The (y_t^d, y_t^r) subsystem is driven by the ''external'' input $g(z_t^d, \theta_y)$ and the (z_t^d, z_t^r) system is driven by external inputs $g(y_t^d, \theta_z)$ and $g(y_t^r, \theta_z)$, respectively, which become identical once the y signals synchronize. Thus the processes described in Sec. II apply directly to the coupled subsystems, except that the aperiodic driving inputs are now coming from another map rather than from a stochastic process.

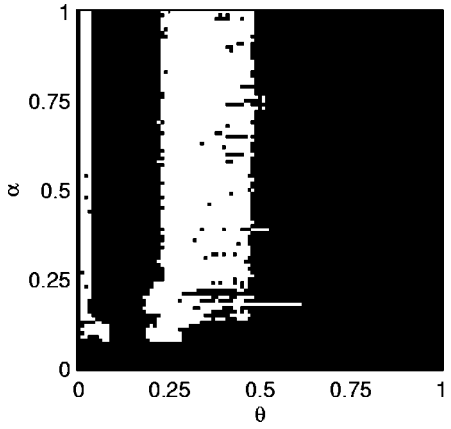

FIG. 4. Dependence on θ and $\alpha=\beta$ of synchronization probability for a pair of coupled oscillators with noise-free coupling, with $\mu_z=\mu_y=7.0$, $A=C=5.0$, and $B=D=1.0$. White indicates that synchronization always occurred in 20 independent runs. See the text for a discussion.

We begin by showing that the system described above synchronizes in the absence of channel noise. The synchronization error in the *y* and *z* variables, respectively, is defined as

$$e^y_{t+1}=y^d_{t+1}-y^r_{t+1}=F_y(e^y_t,y^d_t,z^d_t),$$

$$e^z_{t+1}=z^d_{t+1}-z^r_{t+1}=F_z(e^z_t,e^y_t,y^d_t,z^d_t),$$

and $(e^y,e^y)=(0,0)$, which is an invariant manifold for the system's dynamics, is termed the *synchronization manifold (SM)*. The local stability of the SM along a (y^d_t,z^d_t) trajectory can be evaluated by looking at the transverse conditional Lyapunov exponents (CLE's) for the (e^y_t,e^z_t) system. The Jacobian along the trajectory is given by

$$J=\begin{bmatrix}\partial F_y/\partial e^y & \partial F_y/\partial e^z\\ \partial F_z/\partial e^y & \partial F_z/\partial e^z\end{bmatrix}.$$

Since $\partial F_y/\partial e^z=0$, the eigenvalues of J are simply the diagonal elements, which allows the evaluation of the two transverse CLE's

$$\Lambda_y=\lim_{T\to\infty}\frac{1}{T}\sum_{t=\tau}^{\tau+T-1}\ln|\partial F_y/\partial e^y|, \tag{12}$$

$$\Lambda_z=\lim_{T\to\infty}\frac{1}{T}\sum_{t=\tau}^{\tau+T-1}\ln|\partial F_z/\partial e^z|, \tag{13}$$

where the derivatives are evaluated at $(e^y,e^z)=(0,0)$. Note that, as in the case of one-dimensional maps (Sec. II), the CLE's are expected to be negative in the synchronization regime. However, Λ_y and Λ_z are *not* the Lyapunov exponents of the (y_t,z_t) system and their negativity does not imply a lack of chaos. As we show below, the synchronized trajectory is indeed chaotic in most situations.

To determine whether synchronization actually emerges, we simulated the coupled oscillator system in α-θ space, with $A=C=5.0$, $B=D=1.0$, and $\mu_y=\mu_z=7.0$. As mentioned earlier, we use $\beta=\alpha$ and $\{L,H\}=\{0,1\}$. The results

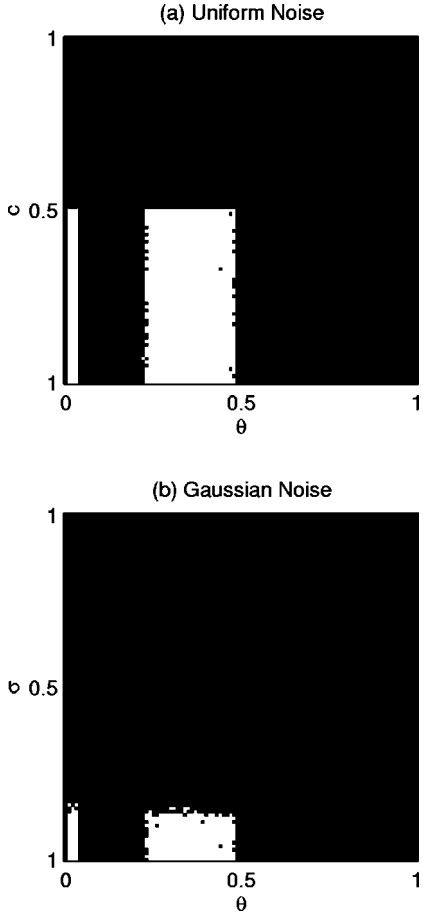

FIG. 5. Dependence on θ of synchronization probability for a pair of coupled oscillators with $\mu_z=\mu_y=7.0$, $A=C=5.0$, $B=D=1.0$, and $\alpha=\beta=1.0$. The channel carrying the synchronizing signal is subject to (a) uniform noise between $\pm c$ and (b) Gaussian noise with variance σ^2. White indicates synchronization with probability 1 over 10 independent runs.

are shown in Fig. 4. There is a distinct parameter range (white region in the figure) where synchronization does emerges reliably.

The dependence of synchronization on α (and β) is as expected. If it is too small, the maps never enter the periodic regime and the CLE's are positive. Once this threshold is met, any value of α and β will do. $L=0$ ensures that the maps always spend time in the mixing regime (if θ is set appropriately). The dependence of synchronization on θ is more complex. Synchronization seems to occur in two strips: one for small θ values and one approximately given by $0.23\leqslant\theta\leqslant 0.50$. The reasons for this pattern are discussed further in Sec. IV.

Finally, we look at whether synchronization occurs as expected in the case when channel noise is present. Figure 5 shows the probability of synchronization for the uniform and Gaussian noise cases for a pair of oscillators with $\mu_y=\mu_z=7.0$, $A=C=5.0$, $B=D=1.0$, $\alpha=\beta=1.0$, and $\{L,H\}=\{0,1\}$. The dependence on the noise strength is as expected, with a sharp cutoff at $c=(H-L)/2$ for uniform noise. For Gaussian noise, synchronization cannot be certain because the probability of suprathreshold noise is nonzero. However, synchronization is obtained with high probability

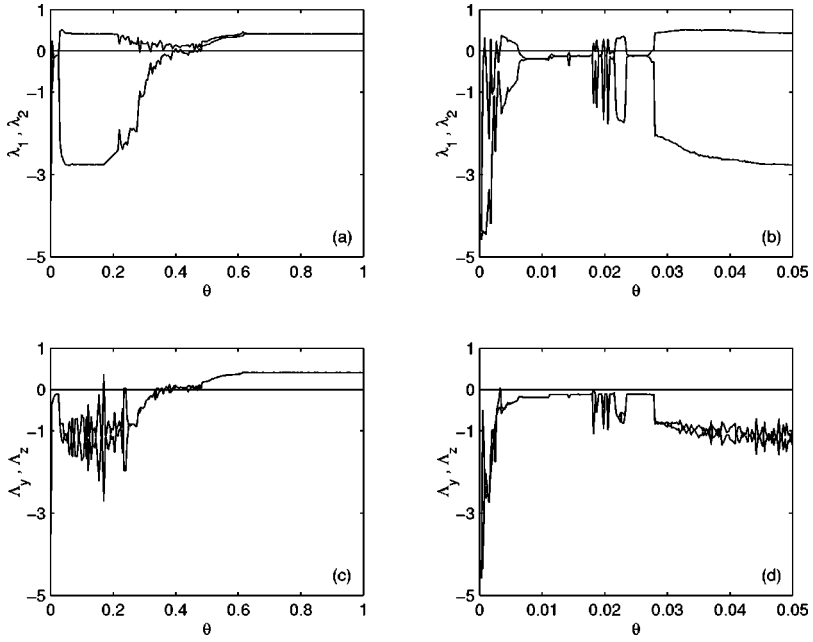

FIG. 6. Graph (a) shows the two Lyapunov exponents λ_1 and λ_2 for the two-dimensional map given by Eqs. (6) and (7), with $\mu_z = \mu_y = 7.0$, $A = C = 5.0$, $B = D = 1.0$, and $\alpha = \beta = 1.0$. Graph (c) shows the CLE's Λ_y and Λ_z in the same situation. Graphs (b) and (d) show the same data as (a) and (c), respectively, with finer resolution over the window $0 \leqslant \theta \leqslant 0.05$.

(i.e., with rare episodes of desynchronization) within a range of c values. The dependence on θ is as for the noise-free case.

IV. DISCUSSION OF RESULTS

In this section we discuss the results shown in Fig. 4, which elucidate the processes underlying the synchronization phenomenon. An important issue that arises is whether the synchronized trajectory obtained in our coupled maps is chaotic at all. This question is particularly relevant because the conditional Lyapunov exponents Λ_y and Λ_z are generally expected to be negative for both drive and response maps in the synchronization regimes. However, this does not mean that the dynamics of the drive and response maps is nonchaotic. To verify this, we numerically calculate [40] the two Lyapunov exponents λ_1 and λ_2 of the map defined by Eqs. (6) and (7) with $\mu_z = \mu_y = 7.0$, $A = C = 5.0$, $B = D = 1.0$, $\alpha = \beta = 1.0$, and different values of θ. We use λ_1 to indicate the larger Lyapunov exponent. Figures 6(a) and 6(b) show that the λ_1 is positive for $\theta > 0.027$ and for many smaller values too. However, the conditional Lyapunov exponents Λ_y and Λ_z do not become positive until $\theta > 0.35$. As θ increases further, the coupling between the y and z maps becomes weaker and at $\theta \leqslant 0.5$ *both* Lyapunov exponents for the map become positive, which is the condition of maximum hyperchaos found in weakly coupled chaotic maps and some other noninvertible systems [41]. Finally, when θ exceeds the maximum value y_t or z_t takes (about 0.613), the y and z maps become uncoupled (since $L = 0.0$) and behave as independent chaotic maps with Lyapunov exponents of about 0.41. Figure 7 shows the bifurcation diagrams for the y and z maps as θ is changed.

A comparison of these results with the synchronization results of Fig. 4 provides insight into the pattern of synchronization.

(i) Synchronization for $0 < \theta \leqslant 0.027$ is actually more complicated than it looks in Fig. 4, which has a resolution of only 0.005 along the θ axis. Figure 6(b) indicates that the $0 < \theta \leqslant 0.027$ region has a finely interwoven structure of chaotic and periodic windows. In the chaotic windows, synchronization occurs as described earlier and the synchronized trajectory is chaotic. However, synchronization can also happen in the periodic windows because of a transient effect. Though the system is not chaotic, the chaotic transient in evolving to the periodic orbit is long enough to allow synchronization, i.e., the system uses the chaos before it disappears. This is supported by the fact that the Lyapunov expo-

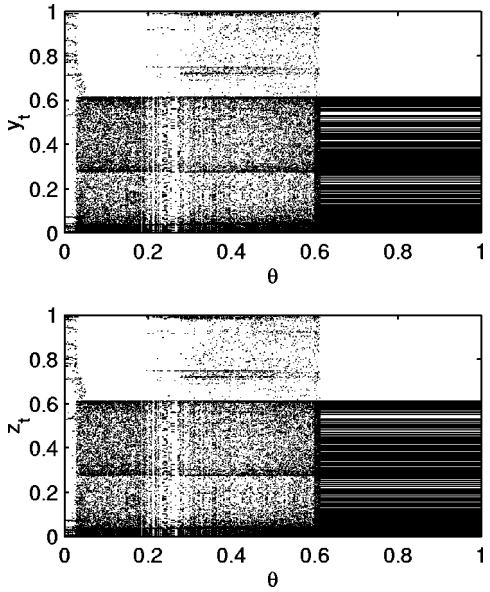

FIG. 7. Bifurcation diagrams for the map given by Eqs. (6) and (7) as θ is varied. The parameters are set as in Fig. 6. Compare the bifurcation diagrams with Fig. 6(a).

nents (LE's) for the system are only weakly negative in the periodic windows, suggesting slow convergence. Of course, the synchronized trajectory obtained in these cases is periodic rather than chaotic.

(ii) The region $0.0.027<\theta<0.23$ has negative CLE's, but a strongly positive λ_1. Also, the CLE's in this region appear to fluctuate strongly with θ [Fig. 6(c)]. We conjecture that the local Lyapunov exponents along some trajectories in this region are too strongly positive to allow synchronization to take hold, which corresponds to a type-(ii) regime in terms of the classification given at the end of Sec. II.

(iii) The band of synchronization for $0.23\leqslant\theta<0.5$ is in fact two regions. For $0.23\leqslant\theta\leqslant0.35$ the CLE's Λ_y and Λ_z are negative and synchronization happens as discussed earlier. This is a type-(iii) regime in terms of the classification of Sec. II. The synchronized trajectory obtained is chaotic because $\lambda_1>0$. However, there is clearly a qualitative change in the system at $\theta\approx0.23$, with λ_1 decreasing slightly (and becoming a more erratic function of θ) and λ_2 increasing rapidly.

At $\theta\approx0.35$ the CLE's Λ_y and Λ_z approach zero and remain close to this value (or slightly positive) until $\theta\approx0.5$. Synchronization still emerges reliably in this region, presumably due to negative local Lyapunov exponents and finite precision. This is a type-(iv) regime in the terminology of Sec. II.

(iv) At $\theta\approx0.5$ there is another clear transition [see Figs. 6(a) and 6(c)] where both LE's and both CLE's jump to significantly positive values and the system displays maximum hyperchaos. This means that there is no volume-contracting direction remaining in phase space. The map has become locally volume expanding and the dynamics is confined purely by the limited range of the tanh() function [41,13]. Since coalescence, by definition, requires contraction, maximally hyperchaotic systems cannot be synchronized by this means and synchronization ceases to occur for $\theta>0.5$.

(v) Finally, at $\theta\approx0.62$ the y and z maps become decoupled because $L=0.0$ and θ exceeds the maximum value taken by z_t and y_t. The maps then evolve as two independent chaotic maps with identical LE's.

V. APPLICATION TO DIGITAL COMMUNICATIONS

The system of coupled oscillators described above can be particularly useful for secure digital communication. In this section we outline a possible system for such an application. It should be noted that this is mainly a pedagogical system used to illustrate the principle and does not include many features (e.g., pre-encryption and redundancy) that could improve its performance, particularly with respect to security.

The system consists of a transmitter and a receiver, both of which are assumed to be digital devices with possibly very high but finite numerical precision. It is also assumed that, within each device, signals can be generated and communicated without noise and that system parameters can be set accurately down to the available precision. All these assumptions are valid for digital systems with programmed functionality. The primary impediment to reliable communication is channel noise, which is inherently analog and independent of the system. The goal of our system is to provide reliable masked communication in the presence of channel noise.

The *information signal* $q_k, k=0,1,2,\ldots,$ takes values 0 or 1, with a pulse width of L discrete-time steps. Thus the *message signal* is given by

$$m_t=q_k, \quad k=\lfloor t/L \rfloor.$$

Each information bit produces L identical message bits and L can be seen as the per bit *chip rate* of the system. The transmitter consists of a drive oscillator with the parameters of the y^d map modulated by the message signal. Such schemes have also been used by other researchers [42–44]. The equations for the transmitter system are given by

$$y^d_{t+1}=\tanh\{\mu_{y_t}[C_t y^d_t+\beta g(z^d_t,\theta_y)]\}-\tanh(\mu_{y_t}D_t y^d_t), \tag{14}$$

$$z^d_{t+1}=\tanh\{\mu_z[Az^d_t+\alpha g(y^d_{t+1},\theta_z)]\}-\tanh(\mu_z B z^d_t). \tag{15}$$

The parameters are modulated as

$$\mu_{y_t}=\mu^*_y(1+\gamma m_t),$$

$$C_t=\frac{\mu^*_y}{\mu_{y_t}}C^*,$$

$$D_t=\frac{\mu^*_y}{\mu_{y_t}}D^*,$$

where γ is a modulation parameter (typically a small value, e.g., 0.01) and μ^*_y, C^*, and D^* are nominal values used in the receiver. The transmitted signal is given by

$$s_t=g(z^d_t,\theta_y).$$

The receiver consists of a response oscillator driven by the received signal $r_t=s_t+\eta_t$, where η_t is channel noise. The equations for the response oscillator are

$$y^r_{t+1}=\tanh\{\mu^*_y[C^*y^r_t+\beta\phi(r_t)]\}-\tanh(\mu^*_y D^* y^r_t), \tag{16}$$

$$z^r_{t+1}=\tanh\{\mu_z[Az^r_t+\alpha g(y^r_{t+1},\theta_z)]\}-\tanh(\mu_z B z^r_t). \tag{17}$$

Note that the z maps for the transmitter and receiver are identical. The y maps are identical when $m_t=0$ but not when $m_t=1$. Essentially, the transmitter is using $g(z^d_t,\theta)$ as the *spreading sequence* [45,46] for the information signal.

Detection is accomplished by constructing the signal

$$\hat{s}_t=g(z^r_t,\theta_z)$$

at the transmitter and then comparing the last N $(<L)$ bits of each L-bit sequence corresponding to an information bit. Thus, for the kth information bit q_k we get the decision variable

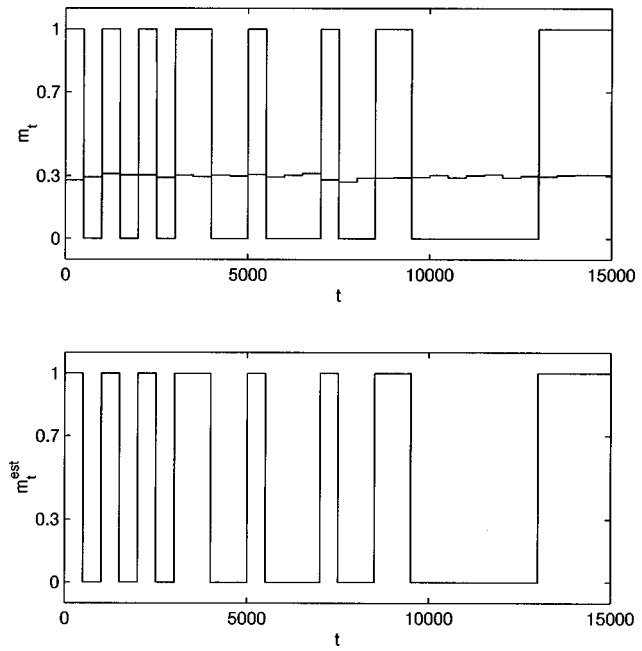

FIG. 8. Transmitted message m_t and decoded message m_t^{est} in the communication system, with $\mu_z=\mu_y=7.0$, $A=C=5.0$, $B=D=1.0$, $\alpha=\beta=1.0$, $L=500$, and $N=20$. The channel carrying the message is subject to uniform noise $\eta\sim U[-0.1,0.1]$. The low-amplitude trace in the upper graph is the mean value of the transmitted signal s_t in the length L window for each message bit. Note its random variation with respect to m_t, rendering it useless for an intruder.

$$d_k=\frac{1}{N}\sum_{t=(k+1)L-N}^{(k+1)L}|s_t-\hat{s}_t|, \quad k=0,1,2,\ldots, \tag{18}$$

and the information bit is detected as

$$\hat{q}_k=\begin{cases}0 & \text{if } d_k<\delta\\ 1 & \text{otherwise.}\end{cases} \tag{19}$$

If L and N are such that synchronization emerges within $L-N$ steps, the system will work. When $q_k=1$, the maps for y_t^d and y_t^r do not match and d_k has a value well above 0. When $q_k=0$, the maps are identical, z_t^d and z_t^r are synchronized within $L-N$ steps, and d_k has a value of 0. One can set δ to a small nonzero value to allow some margin of error. Also, making N longer without violating the requirement on $L-N$ improves detection because brief episodes of intermittent synchronization cannot cause errors. Figure 8 shows an example of successful decoding by the proposed system in the presence of uniform channel noise $\eta\sim U[-0.1,0.1]$. A more detailed evaluation of the system's performance will be presented elsewhere.

The principal aim of the communication system above is to make the transmitted signal as invariant as possible to the information it carries, so that an eavesdropper who obtains the signal cannot recover the information. Four features of the system aid in this.

(i) The digital nature of s_t makes the application of reconstruction methods such as delay-coordinate embedding difficult [47–49].

(ii) The map producing the transmitted signal $f(z_t^d)$ is not directly modulated by the message. Rather, the map driving it, $f(y_t^d)$, undergoes the actual modulation, making the dependence of the transmitted signal on the modulation more complex.

(iii) The modulation of $f(y_t^d)$ is specified such that, in the absence of the $\beta g(z_t^d,\theta)$ drive, the maps would be identical for $m_t=0$ and $m_t=1$. This ensures that the statistics of the y_t^d signal produced in the two cases are extremely similar and so, as a result, are those of s_t. This is especially true if γ is chosen small. We use a value of $\gamma=0.01$.

(iv) The signals produced by the transmitter and receiver are extremely sensitive to changes in parameter values. This makes it very difficult for an intruder to reconstruct the system with sufficient accuracy. At the same time, it also puts stringent requirements on legitimate transmitters and receivers to match parameters very accurately. Such requirements are standard in encrypted communication systems [50–52].

While these features certainly help to make the system secure, we do not claim that this meets the standards necessary for secure communications in practice. Our aim is to elucidate the principle with the simplest possible system. Other enhancements such as encryption can be used to increase security further [52].

One question that may be raised is whether the method we describe is more useful than existing ones based on standard random number generators. While every method has its strengths and weaknesses, we believe our method is interesting because it removes the need for presynchronization between the transmitter and receiver. Current spread spectrum methods [45,46] use identical modulated wave forms (spreading sequences) for every information bit. However, this method is not very secure because the same sequence is used repeatedly, providing greater opportunity for an intruder to estimate it. It would be much better to use nonrepeating spreading sequences for every bit, but that would require the receiver to know this sequence too. By providing a self-synchronizing aperiodic sequence to carry the message, our scheme, as well as other methods based on chaotic synchronization, provides an elegant solution to this problem.

VI. CONCLUSION

In conclusion, we have demonstrated that identical unidirectionally connected chaotic oscillators can be synchronized even when the channel carrying the coupling signal is noisy. This is because synchronization does not require precise signal values, but depends only on gross signal statistics, which allows us to use a digitized coupling. We have also outlined a prototypical secure communication system based on our scheme.

ACKNOWLEDGMENTS

The authors would like to thank Xin Wang, Tao Yang, Chai Wah Wu, Tom Carroll, Kevin Short, and Mingzhou Ding for providing reprints of their work. This work was partially supported by a grant from the Ohio Board of Regents.

[1] L.M. Pecora and T.L. Carroll, Phys. Rev. Lett. **64**, 821 (1990).
[2] L.M. Pecora and T.L. Carroll, Phys. Rev. A **44**, 2374 (1991).
[3] L. Kocarev and U. Parlitz, Phys. Rev. Lett. **74**, 5028 (1995).
[4] U. Parlitz, L. Kocarev, T. Stojanovski, and H. Preckel, Phys. Rev. E **53**, 4351 (1996).
[5] J.H. Peng, E.J. Ding, M. Ding, and W. Yang, Phys. Rev. Lett. **76**, 904 (1996).
[6] T. Yamada and H. Fujisaka, Prog. Theor. Phys. **70**, 1240 (1983).
[7] A. Pikovsky and P. Grassberger, J. Phys. A **24**, 4587 (1991).
[8] A. De Angeli, R. Genesio, and A. Tesi, IEEE Trans. Circuits Syst., I. Fundam. Theory Appl. **42**, 54 (1995).
[9] L.S. Tsimring and M.M. Sushchik, Phys. Lett. A **213**, 155 (1996).
[10] J. Güémez and M.A. Matías, Physica D **96**, 334 (1996).
[11] A.S. Dmitriev, M. Shirokov, and S.O. Starkov, IEEE Trans. Circuits Syst., I: Fundam. Theory Appl. **44**, 919 (1997).
[12] M. M. Sushchik, Jr., N.F. Rulkov, and H.D.I. Abarbanel, IEEE Trans. Circuits Syst., I: Fundam. Theory Appl. **44**, 867 (1997).
[13] L.M. Pecora, T.L. Carroll, G. Johnson, and D. Mar, Phys. Rev. E **56**, 5090 (1997).
[14] T.L. Carroll and L.M. Pecora, IEEE Trans. Circuits Syst., I: Fundam. Theory Appl. **45**, 656 (1998).
[15] F.E. Udwadia and N. Raju, Physica D **111**, 16 (1998).
[16] K. Kaneko, Physica D **37**, 60 (1989).
[17] K. Kaneko, Physica D **41**, 137 (1990).
[18] J.M. Kowalski, G.L. Albert, and G.W. Gross, Phys. Rev. A **42**, 6260 (1990).
[19] G. Keller, M. Künzle, and T. Nowicki, Physica D **59**, 39 (1992).
[20] N. Nakagawa and Y. Kuramoto, Prog. Theor. Phys. **89**, 313 (1993).
[21] T. Kapitaniak, Phys. Rev. E **47**, R2975 (1993).
[22] V.I. Nekorkin, V.A. Makarov, V.B. Kazantsev, and M.G. Veralde, Physica D **100**, 330 (1997).
[23] L.M. Pecora, Phys. Rev. E **58**, 347 (1998).
[24] S.C. Venkataramani, B.R. Hunt, and E. Ott, Phys. Rev. E **54**, 1346 (1996).
[25] H.L. Yang and E.J. Ding, Phys. Rev. E **54**, 1361 (1996).
[26] D.J. Gauthier and J.C. Bienfang, Phys. Rev. Lett. **77**, 1751 (1996).
[27] A.A. Minai and T. Anand, Phys. Rev. E **57**, 1559 (1998).
[28] A.A. Minai and T. Anand, in *Proceedings of the International Joint Conference on Neural Networks 98* (IEEE, Piscataway, NJ, 1998), pp. 1466–1471.
[29] X. Wang, Complex Syst. **5**, 425 (1991).
[30] X. Wang, Ph.D. thesis, University of Southern California, 1992 (unpublished).
[31] A.A. Minai and T. Anand, Biol. Cybern. **79**, 87 (1998).
[32] L. Yu, E. Ott, and Q. Chen, Phys. Rev. Lett. **65**, 2935 (1990).
[33] L. Yu, E. Ott, and Q. Chen, Physica D **53**, 102 (1991).
[34] A.S. Pikovsky, Phys. Lett. A **165**, 33 (1992).
[35] L. Longa, E.M.F. Curado, and F.A. Oliviera. Phys. Rev. E **54**, R2201 (1996).
[36] L. Longa, S.P. Dias, and E.M.F. Curado. Phys. Rev. E **56**, 259 (1997).
[37] Y.-C. Lai, Phys. Rev. E **54**, 321 (1996).
[38] E. Ott and J.C. Sommerer, Phys. Lett. A **188**, 39 (1994).
[39] Y. Maistrenko, V.L. Maistrenko, A. Popovich, and E. Mosekilde, Phys. Rev. E **57**, 2713 (1998).
[40] K.T. Alligood, T.D. Sauer, and J.A. Yorke (Springer-Verlag, New York, 1997).
[41] J.W. Shuai, Z.X. Chen, R.T. Liu, and B.X. Wu, Phys. Rev. E **56**, 890 (1997).
[42] K.M. Cuomo, A.V. Oppenheim, and S.H. Strogatz, IEEE Trans. Circuits Syst., II: Analog Digital Signal Process. **40**, 626 (1993).
[43] T. Yang and L.O. Chua, Int. J. Bifurcation Chaos Appl. Sci. Eng. **6**, 2653 (1996).
[44] T. Yang and L.O. Chua, IEEE Trans. Circuits Syst., I: Fundam. Theory Appl. **43**, 817 (1996).
[45] S. Moshavi, IEEE Commun. Mag. **34**, 124 (1996).
[46] P.G. Flikkema, IEEE Signal Process. Mag. **14**, 26 (1997).
[47] K.M. Short, Int. J. Bifurcation Chaos Appl. Sci. Eng. **4**, 959 (1994).
[48] G. Peréz and H.A. Cerdeira, Phys. Rev. Lett. **74**, 1970 (1995).
[49] K.M. Short, Int. J. Bifurcation Chaos Appl. Sci. Eng. **6**, 367 (1996).
[50] K.S. Halle, C.W. Wu, M. Itoh, and L.O. Chua, Int. J. Bifurcation Chaos Appl. Sci. Eng. **3**, 469 (1993).
[51] T. Yang, C.W. Wu, and L.O. Chua, IEEE Trans. Circuits Syst., I: Fundam. Theory Appl. **44**, 469 (1997).
[52] A.A. Minai and T.D. Pandian, Chaos **8**, 621 (1998).